

U H E neutralinos signatures: selectron/squark resonances in telescopes, and sneutrino bursts in the U niverse

A nindya D atta, D aniele F argion, and B arbara M ele ¹

INFN, Sezione di Roma, and
D ip. di F isica, Universita La Sapienza, P . le A . M oro 2, I-00185, Rom e, Italy.

A bstract

In the Top-down scenarios, the decay of super-heavy particles ($m \sim 10^{16}$ GeV), situated in dark-matter halos not very far from our Galaxy, can explain the ultra-high-energy (UHE) cosmic-ray spectrum beyond the Griesen-Zatsepin-Kuzmin (GZK) cut-off. In case the dynamics of this decay is governed by the minimal supersymmetric standard model, a major component of the UHE cosmic-ray flux at PeV-EeV energies could be given by the lightest neutralino $\tilde{\chi}_1^0$, that is the lightest stable supersymmetric particle. Then, the signal of UHE $\tilde{\chi}_1^0$'s on earth might emerge over the interactions of a comparable neutrino component. We compute the event rates for the resonant production of right selectrons (\tilde{e}_R) and right squarks (\tilde{q}_R) in mSUGRA, when UHE neutralinos of energy $E > 10^5$ GeV scatter off electrons and quarks in an earth-based detector like IceCube. The production rates and decay widths into the same initial particles $\tilde{\chi}_1^0 e$; $\tilde{\chi}_1^0 q$ turn out to be nearly model independent (the resonance and neutralino physical masses being the only relevant parameters) for the neutralino-electron scattering, and also for the neutralino-nucleon scattering, whenever gluinos are heavier than squarks. We compare the expected number of supersymmetric events with the rates corresponding to the Glashow W resonance and the continuum UHE N scattering for realistic power-law spectra. We find that the supersymmetric event rate can reach a few tens for a one-year exposure in IceCube. Finally, we note that UHE neutralinos at much higher energies (up to hundreds ZeV) may produce sneutrino ($\tilde{\nu}$) resonances by scattering off relic neutrinos in the Local Group hot dark halo. The consequent $\tilde{\nu}$ burst into hadronic final states could mimic a Z-burst event, but with a quite smaller conversion efficiency.

1 Introduction

The presence of a ultra-high-energy (UHE) component in the cosmic-ray spectra beyond the GZK-cut-off [1], as revealed initially by the experiment Fly's Eye [2], subsequently by AGASA [3], and marginally by Hires [4], is presently an open problem in high-energy astrophysics. The highest-energy particles in the cosmic-ray spectrum are apparently protons rather than photons, because of their characteristic hadronic-shower uorescence light shapes. Beyond the GZK energies, protons, slowed down by the cosmic Black Body Radiation, have energy-loss length well below 50 Mpc. This implies that possible sources of these extremely-high-energy particles should be within our Galaxy, or inside our Local Group of Galaxies or nearby Clusters. However, there are no such powerful sources in Milky Way or nearby Virgo

¹E-mail: A nindya D atta@ rom a1 .inf n .it, D aniele F argion@ rom a1 .inf n .it, B arbara M ele@ rom a1 .inf n .it

Group, that are correlated with the arrival map of the UHE cosmic rays (UHECR). There is a timid, and yet unconfirmed, clustering of AGASA data along the Super-Galactic Plane, not sufficient to probe the UHECR confinement in observable GZK volumes. On the contrary, UHECR events exhibit isotropy, a signature reminiscent of most distant cosmic edges. It is not clear whether the UHECR spectrum is really showing a GZK cut-off [3, 4]. In order to make our UHECR understanding even more confused, there are now first evidences of clustered UHECR events by AGASA correlated with known BL Lacs sources [5]. This UHECR-BL Lacs connection calls for the UHE Blazing Jet of active galactic nuclei (AGN) as a source of particle acceleration. Those BL Lacs sources are mostly at distances above GZK lengths.

Although the GZK puzzle is still experimentally not completely settled, in the past and also recently, there have been quite a few suggestions about possible sources and mechanisms for accelerating particles to such extreme energies [6, 7].

A class of proposals, generically called Top-down scenarios, tries to explain the high-energy part of the spectrum through the decay of super-massive particles ($m \gtrsim 2 \cdot 10^{16}$ GeV) [8, 9, 10, 11, 12], or by their eventual binary collapse and annihilation in place of time-tuned decays [13]. These particles are generally predicted in Grand Unified Theories (GUT). Their decay lifetime should be comparable with the present age of the Universe, so that their decay products would give rise today to the highest energy part of the cosmic-ray spectrum. Also topological defect decays can give rise to the UHECR primaries [6]. In any case, the decay dynamics of the super-heavy particles is controlled by the model assumed for particle interactions. In the standard model (SM), the decay after fragmentation usually results into photons, neutrinos and hadrons. In supersymmetry (SUSY), UHE secondary stable neutralinos ($\tilde{\chi}_1^0$) may be born, too [9, 10, 11, 12].

The minimal supersymmetric standard model (MSSM) is a well motivated extension of the standard model of elementary particles [14]. SUSY stabilizes the Higgs-boson mass under radiative corrections by introducing an entire spectrum of supersymmetric partners for the SM particles. The MSSM predicts a stable weakly-interacting heavy neutral particle, called neutralino ($\tilde{\chi}_1^0$), which can be also a good candidate for cold dark matter². If the masses of supersymmetric particles are at the TeV scale (as needed to stabilize the Higgs-boson mass), we expect to discover them in a few years at the CERN LHC [15]. In the case SUSY is the correct theory of particle interactions, it will govern also the decays of super-heavy particles. In [10, 11, 12], the super-heavy particle decays in the MSSM extension of the SM have been investigated in detail. These decays would involve the entire spectrum of SUSY partners. At the end of the decay chain, one would be left with a spectrum (calculable in the MSSM) of all the stable particles, that is SM particles plus stable neutralinos. Hence, a crucial prediction of these models is the presence of neutralinos in the UHECR spectrum produced by super-heavy objects.

Another possible explanation for the GZK paradox considers relic light neutrinos as a calorimeter in resonance with incoming UHE (ZeV's) neutrinos. The latter may come freely from distances above GZK from far BL Lacs or gamma ray bursts (GRB). They may also arise from topological defects spread all over dark halos (Galactic or extra-galactic). This model, the so-called Z-burst model [16] will be discussed in the following in view of a new and analogous sneutrino-burst model.

UHECR may also arise from Jet accelerations in AGN, GRB, and even in local soft gamma repeaters [6]. In these Jets the primary particles should be made of common SM matter in case the Jet invariant mass is less than a few tens GeV. However, in UHE thick accelerators (beam-dumped Jets) whose center-of-mass energy exceeds hundreds of GeV or

² In general, in the MSSM, there are 4 neutralinos. Here, we are talking about the lightest one $\tilde{\chi}_1^0$.

TeV, secondaries may contain also relevant components of SUSY neutralinos. These TeV neutralinos will be naturally boosted in the laboratory at UHE (PeV–ZeV).

According to the discussion above, we shall assume in this study either a hard neutralino spectrum $\propto E^{-\frac{3}{2}}$ (as from GUT-relics Fragmentation), or a softer Fermi-like spectrum $\propto E^{-2}$ (as from AGN/GRB Jets). We shall not consider a much harder Z-burst-like spectrum ($\propto E^{-1}$) that is usually used in different context, although such a spectrum could be of relevance for a sneutrino-burst model.

One of the major goals for the upcoming UHECR experiments (like Amanda, IceCube, Antares, Nestor) is to verify these predictions. In [17], the possible signatures of up-going UHE neutralinos in the future satellite-based detector EUSO [18] have been investigated. The resonant production of quite heavy squarks ($m \approx 0.8 - 1.2$ TeV) in the ν_1^0 scattering on nucleons in the earth's atmosphere, after crossing all the earth volume, has been considered. Heavy squarks are selected so that the neutralino interaction cross sections are moderate, and the neutralino flux is not completely stopped by the earth screen (while the corresponding neutrino background does not survive the passage through the earth). An analogous process leading to a smaller neutrino earth opacity has been also considered earlier, while discussing the up-going neutrinos [9]. Note that, in EUSO, the UHE neutralino interaction in the atmosphere is polluted by more abundant up-going horizontal air-showers induced by UHE earth skinning in the terrestrial crust [20].

In the present article, we will focus on the interaction of the highest energy neutralinos with both electrons and nucleons in a earth-based detector like IceCube [21]. In particular, we will study the possibility to detect the resonant production of the SUSY partners of electrons and quarks, when their masses are not too far from the present experimental limits derived from direct searches at high-energy colliders ($m_e > 100$ GeV for selectrons [22], $m_q > 300$ GeV for squarks³ [23]).

Neutralinos with appropriate energy can produce a right/left selectron (e_R/e_L) resonance in the detector via the scattering on the detector electrons

$$\nu_1^0 + e \rightarrow e_{R/L} \rightarrow X$$

(see Fig. 1). Here, X stands for some visible final state arising from the $e_{R/L}$ decay, that will be eventually revealed by the detector.

The kinematics and signature is somehow similar to the W resonant production in UHE antineutrino-electron scattering [24]

$$\bar{\nu}_e + e \rightarrow W \rightarrow X;$$

occurring at the Glashow resonant energy $E = \frac{M_W^2}{2m_e} \approx 6.4$ PeV.

Since we do know the exact characteristics of this channel (like all its hadronic and electromagnetic showering and its final visible energies), the corresponding events will be used to calibrate the SUSY resonance observation.

Right/left-squark ($q_R=q_L$) resonances can be produced through the neutralino scattering on the quarks in the detector nucleons

$$\nu_1^0 + q \rightarrow q_{R/L} \rightarrow X;$$

Although, at the partonic level, this process has the same resonant structure as the selectron channel, due to the quark momentum spread inside the nucleon, the cross-section resonance peak is smeared, and the ν_1^0 incident-energy resonant characteristics are lost.

³Even lighter squarks are allowed for $m_{\tilde{g}} = m_q$.

The background coming from the UHE ν -neutrino interaction with nucleons ($\nu + q \rightarrow X$) by t-channel processes could create a major continuous background overlapping or overshadowing the squark signal. In the following, after computing the relevant $\sigma_{\nu N}$ event rates, we will address the issue of disentangling the SUSY signal from the SM resonant and continuous background given by the competitive UHE neutrinos.

Higher-energy neutralinos [with $E_{\tilde{\chi}^0_1} = (2m_{\tilde{\chi}^0_1})$] could interact with light relic neutrinos in the Local Group or Super-Galactic Plane, and produce sneutrino $\tilde{\nu}$ resonances in the process

$$\tilde{\chi}^0_1 + \nu \rightarrow \tilde{\nu} + X;$$

The following sneutrino decay into final states containing hadrons can in principle mimic a Z-burst event [16]. In this paper, we will go through a $\tilde{\nu}$ -burst scenario. We will find that it is in general less effective than the Z-burst model in solving the GZK paradox.

While calculating the neutralino scattering cross-sections, we will stick to a particular model of SUSY breaking, namely the minimal supergravity mediated model (mSUGRA) [25]. The mSUGRA and its variants are theoretically well motivated. The parameter space of mSUGRA is characterized by five quantities: m_0 and $m_{1/2}$, the universal scalar and gaugino masses, respectively; A_0 , the universal trilinear scalar coupling (all taken at the scale of grand unification); $\tan \beta$, the ratio of the vacuum expectation values of the two Higgs doublets; the sign of μ , the Higgs mixing parameter ($W_3 = H_1 H_2$, where H_1, H_2 are the two Higgs superfields in the superpotential W). While the sign of μ is arbitrary, its magnitude is determined by requiring the radiative electro-weak symmetry breaking.

In most of the mSUGRA parameter space, the lightest neutralino is practically a bino \tilde{B} , the superpartner of the U(1) gauge field⁴. This is particularly important for $\tilde{\chi}^0_1$ being a good candidate for cold dark matter [26]. Then, the right slepton and right squark can be maximally coupled to the lightest neutralino, and resonant $\tilde{\chi}^0_1 f \rightarrow \tilde{f}_R$ cross sections are in general enhanced with respect to $\tilde{\chi}^0_1 f \rightarrow \tilde{f}_L$ cross sections (where $f = e, q$).

We will then restrict our study to the right-scalar resonant production and decay into the same initial particles $\tilde{\chi}^0_1 f$. The corresponding production rates will turn out to be model independent, the only critical parameters being the physical masses of the particle involved in the process (that is the resonance and neutralino masses, $m_{\tilde{f}_R}$ and $m_{\tilde{\chi}^0_1}$).

In any case, one should keep in mind that the model predicts further new channels associated to the left scalar resonances (sort of twin shadows of the right scalars) whose rate is in general suppressed with respect to the right scalar by both the lower (and in general more model-dependent) relevant decay branching fractions (see Section 3), and the heavier resonance masses (since in general $m_{\tilde{f}_L} > m_{\tilde{f}_R}$).

The neutralino energies that are relevant for the resonant reactions $\tilde{\chi}^0_1 q \rightarrow q$, $\tilde{\chi}^0_1 e \rightarrow e$, $\tilde{\chi}^0_1 \nu \rightarrow \nu$ are strictly determined by the resonance and target masses [$E_{\tilde{\chi}^0_1} = (2m_{\text{target}})$], that is

$$E_{\tilde{\chi}^0_1} > \frac{m_q^2}{2m_p} \sim 10^5 \text{ GeV}; \quad (1)$$

$$E_{\tilde{\chi}^0_1} > \frac{m_e^2}{2m_e} \sim 10^6 \sim 10^8 \text{ GeV}; \quad (2)$$

$$E_{\tilde{\chi}^0_1} > \frac{m_{\tilde{\nu}}^2}{2m_{\tilde{\nu}}} \sim 10^{14} \text{ GeV}; \quad (3)$$

respectively, where $m_p, m_e, m_{\tilde{\nu}}$ are the proton, electron, relic-neutrino masses.

⁴ In general, a neutralino is a linear combination of the two Higgs superpartners (\tilde{H}_1, \tilde{H}_2), a \tilde{W}_3 (wino) and a \tilde{B} (bino).

The plan of this paper is the following. In Section 2, we discuss our assumptions on the UHE-neutralino spectrum in two main scenarios, i.e. the GUT-relics Fragmentation power law, and the Fermi-like at power law. In Section 3, we present the cross-sections for the UHE-neutralino interaction with electrons and quarks leading to selectron and squark resonances. In Section 4, we present the event rates for the selectron and squark resonant production by UHE $\tilde{\chi}_1^0$ for a 1-km³ ice detector. They will then be compared with the number of events coming from the Glashow resonance $e e \rightarrow W$, and from the $(\bar{\nu} \nu)$ nucleon interaction via charged- and neutral-current processes, assuming comparable UHE-neutrino and neutralino spectra. We also address the issue of disentangling the SUSY events in the detector by looking at their peculiar energy spectrum and hence for visible decay products. In Section 5, we will discuss a possible γ -burst scenario, corresponding to the resonant interaction of UHE $\tilde{\chi}_1^0$'s with light relic neutrinos in the Local Group or SuperCluster hot dark halos. Finally, in Section 6, we present our conclusions.

2 The UHE-neutralino spectrum

As for our assumptions for the neutralino flux in the UHECR, although we are primarily motivated by models of SUSY-driven decays of super-heavy particles, we will not be strictly using the corresponding neutralino spectrum [11, 12]. Instead, we will try to keep our study as independent as possible of the particular origin of the neutralino component in the UHECR. Hence, we will follow a phenomenological and model-independent approach, only guided by present and projected experimental limits on UHECR neutrino fluxes. Neutrinos and neutralinos of comparable energies, while interacting with matter, will produce somewhat similar signals in an earth-bound detector. In general, neutralino-interaction rates are expected to be smaller than the neutrino ones. This consequently implies less stringent experimental bounds on the neutralino fluxes compared to the neutrino fluxes [7]. Although there would be some room for a more abundant incoming UHE-neutralino flux compared to the neutrino ones, we will assume, for the sake of simplicity and with a conservative attitude, comparable UHE fluxes, that is $\Phi_{\tilde{\chi}} \sim \Phi_{\nu}$. For the energies we are interested in for selectron and squark resonances (i.e., $E = 10^5 - 10^9$ GeV), Amaldi gives some experimental limit on neutrino fluxes in the lowest energy range [27], while for the highest edges, some upper bound on the UHECR neutrino flux comes from AGASA [3] and Fly's Eye [2]. More severe bounds were recently put at the highest neutrino energies by ICEBERG [28]. According to the latter experiments, $E^2 \frac{dN}{dE} \leq 10^{-7} \text{ GeV cm}^{-2} \text{ s}^{-1} \text{ sr}^{-1}$, for the $\nu_\mu + \bar{\nu}_\mu$ component in the PeV's energy range. Hence, assuming comparable interaction strength for neutrinos and neutralinos, one can adopt a neutralino flux as high as the latter, while weaker neutralino interactions would allow even higher spectra.

Then, as neutralino flux we have used, quite conservatively, two different power laws, i.e. a Fragmentation power law :

$$E^2 \frac{dN}{dE} = 10^{-7} \text{ GeV cm}^{-2} \text{ s}^{-1} \text{ sr}^{-1} \left(\frac{E}{10^7 \text{ GeV}} \right)^{0.5} \quad (4)$$

and a Fermi at power law (as in a shock-wave plasma either in SuperNovae-GRBs or in AGN Jets):

$$E^2 \frac{dN}{dE} = 10^{-7} \text{ GeV cm}^{-2} \text{ s}^{-1} \text{ sr}^{-1} \quad (5)$$

A few comments are in order. Since the limits on the neutrino flux discussed above holds for just one neutrino flavor (i.e., the $\nu_\mu + \bar{\nu}_\mu$ component), by adopting the neutralino fluxes

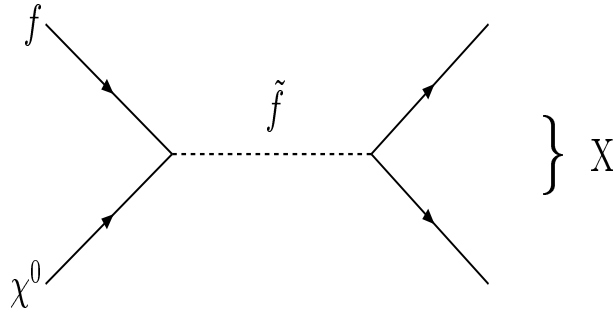


Figure 1: Feynman diagram of the process $\tilde{\chi}_1^0 + f \rightarrow \tilde{f} \rightarrow X$, where f can be an electron, a quark or a neutrino.

in eq. (4) and eq. (5) we will assume that the neutralino flux is comparable with the flux of just one neutrino species, i.e. $\Phi_{\tilde{\chi}_1^0} \sim \Phi_{\nu_i}$ ($i = e, \mu, \tau$). This hypothesis could be quite conservative, since models of superheavy-particle decays can give rise to neutralino fluxes comparable with the sum of all the neutrino components [12]. Secondly, the flux shape in eq. (4) is quite similar to the one resulting from the decay of a superheavy particle of mass 10^{12} GeV primarily into 5 quarks [12]⁵, although the latter is approximately two orders of magnitude smaller than the one in eq. (4) at $E = 10^9$ GeV. Models of UHECR fluxes arising from superheavy particle decays have been mainly motivated by the GZK puzzle. Consequently, the maximum of the neutralino distribution, whose position is directly connected to the superheavy particle mass, has been pushed in [12] to quite large energy values in order to explain the GZK puzzle. Reasonable sources of the neutralino flux in our case could arise from lighter superheavy particles (as considered for instance in [11]), and should be enhanced in the energy range of $10^7 - 10^8$ GeV. In that case, according to the treatment in [12], the normalization in eq. (4) could be quite natural.

In the following, we will calculate SUSY event rates by assuming either the Fragmentation and the Fermi at spectrum for the neutralino flux.

3 Resonant cross sections for UHE neutralino interactions with matter

UHE neutralinos with proper energy will interact with the electrons and quarks inside the detector, and produce selectron or squark resonances via $\tilde{\chi}_1^0 + (e, q) \rightarrow (\tilde{e}, \tilde{q}) \rightarrow X$ (see the Feynman diagram in Fig. 1, where f is either a lepton or a quark). The symbol X stands for a particular \tilde{f} decay final state.

Near the resonance, the cross-section of the process can be written in terms of the particle masses and the $\tilde{\chi}_1^0$ center-of-mass (c.m.) energy s in the Breit-Wigner approximation

$$\sigma(s) = 2 \frac{1}{k} \frac{s}{(s - m_{\tilde{f}}^2)^2 + m_{\tilde{f}}^2 \Gamma_{\tilde{f}}^2} B(\tilde{f} \rightarrow \tilde{\chi}_1^0 f) B(\tilde{f} \rightarrow X) : \quad (6)$$

In the equation above, $m_{\tilde{f}}$ is the slepton/squark mass, $\Gamma_{\tilde{f}}$ is its total decay width, and $B(\tilde{f} \rightarrow \tilde{\chi}_1^0 f)$, $B(\tilde{f} \rightarrow X)$ are their decay branching fractions ($B(\tilde{f} \rightarrow ::) = (\tilde{f} \rightarrow ::)/\Gamma_{\tilde{f}}$) into the final states $\tilde{\chi}_1^0 f$, X , respectively. The modulus of the c.m. 3-momentum of the

⁵The flux in [12] goes down with the energy as $E^{-1.3}$.

initial particles k can be expressed as

$$k \cdot j = \frac{m_{\tilde{f}}^2 - m^2}{2m_{\tilde{f}}} \quad (7)$$

where m is the neutralino mass. Then, the cm. energy s is related to the incident neutralino energy E in the laboratory by

$$s = m^2 + 2m_{\tilde{f}}E; \quad (8)$$

where $m_{\tilde{f}}$ is the target mass. On the resonance ($s = m_{\tilde{f}}^2$), the neutralino energy is then

$$E^{\text{peak}} = \frac{m_{\tilde{f}}^2 - m^2}{2m_{\tilde{f}}}; \quad (9)$$

which sets the neutralino energy scales relevant to our study: PeV's-EeV's for squarks and selectrons, and hundreds of ZeV's for sneutrino bursts.

The peak cross section $\sigma^{\text{peak}}(s = m_{\tilde{f}}^2)$ can be obtained from eq. (6) in a straightforward way :

$$\sigma^{\text{peak}} = \frac{8}{m_{\tilde{f}}^2} @ \frac{m_{\tilde{f}}^2}{m_{\tilde{f}}^2 - m^2} A^0 B(\tilde{f} \rightarrow \tilde{f}_1^0) B(\tilde{f} \rightarrow X): \quad (10)$$

In the naive event-rate estimate, a crucial quantity will be given by the product $\sigma^{\text{peak}}_{\tilde{f}}$, the resonance peak cross section times its total decay width (the latter setting the actual energy width of the resonance curve), that in general will depend on all the 5 mSUGRA parameters.

In this analysis, we will concentrate on some important scenarios where a relatively small parameter dependence is left in the cross sections, apart from the leading $m_{\tilde{f}}$ mass dependence. In particular, in these (quite general) scenarios, there will be little parameter dependence in the \tilde{f} decay branching fractions into both the initial \tilde{f}_1^0 and $\text{na}X$ states, these branching fractions being the crucial parameters entering σ^{peak} . These conditions most naturally realize in processes where the resonance is maximally coupled to the initial \tilde{f}_1^0 state (that is $B(\tilde{f} \rightarrow \tilde{f}_1^0) \simeq 1$), and, at the same time, one considers as decay products just the same initial \tilde{f}_1^0 particles, in the process

$$\tilde{f}_1^0 + \tilde{f} \rightarrow \tilde{f} \rightarrow \tilde{f}_1^0 + \tilde{f}: \quad (11)$$

Then, the corresponding peak cross section becomes parameter independent in mSUGRA

$$\sigma^{\text{peak}} \simeq \frac{8}{m_{\tilde{f}}^2} @ \frac{m_{\tilde{f}}^2}{m_{\tilde{f}}^2 - m^2} A^0: \quad (12)$$

In the same scheme, also the parameter dependence of the total width $\Gamma_{\tilde{f}}$ will be mainly restricted to phase-space mass effects.

A natural framework where to implement the above picture is given by the right selectron and right squark resonances in mSUGRA. In mSUGRA, the right selectron \tilde{e}_R is in general one of the lightest superpartner, and the lightest neutralino is mainly a bino \tilde{B} . For conserved R parity, the dominant \tilde{e}_R decay channel is $\tilde{e}_R \rightarrow \tilde{e}_1^0$, with a corresponding branching fraction of almost 100%. On the other hand, the left selectron \tilde{e}_L is usually more coupled to the second lightest neutralino $\tilde{0}_2$ and to the lightest chargino $\tilde{1}^+$. Hence, when allowed by phase-space, the decays $\tilde{e}_L \rightarrow \tilde{0}_2 e$ and $\tilde{e}_L \rightarrow \tilde{1}^+ e$ tend to be dominant. Therefore, $B(\tilde{e}_L \rightarrow \tilde{e}_1^0)$ is in general not very large, and depletes the peak $\tilde{e}_1^0 \rightarrow \tilde{e}_L \rightarrow X$ cross section.

On the other hand, for the right selectron, according to eq. (10), the peak cross-section is maximized when looking to at a \tilde{e}_1^0 final state in the channel

$$\tilde{e}_1^0 + e \rightarrow \tilde{e}_R \rightarrow \tilde{e}_1^0 + e; \quad (13)$$

being $m_{\tilde{e}_R}$ and $m_{\tilde{e}_1^0}$ the only relevant parameters that govern the cross section, as from eq. (12). Hence, the dominant signature of the resonant interaction of a neutralino with an electron in the detector will be an energetic electron carrying away a fair fraction of the initial neutralino resonant energy. Then, the \tilde{e}_R signature will be totally characterized by an electromagnetic showering, while the Glashow W resonance will be mostly proceeding through hadronic channels.

For the squark sector, that is relevant in the neutralino interactions with the nuclei of the detector, a similar discussion holds regarding the branching fractions of the right and left squarks into q_1^0 (in particular, one has $B(\tilde{q}_R \rightarrow q_1^0) = 1$, $B(\tilde{q}_L \rightarrow q_{1,2}^0) = 2/3$, and $B(\tilde{q}_L \rightarrow q_2^0) = 1/3$), unless the gluino is lighter than the squark. In the latter case, the strong interacting decay $\tilde{q}_{R,L} \rightarrow q\tilde{g}$ is by far dominant, and the squark coupling to the initial q_1^0 is suppressed (due to the small branching fraction $B(\tilde{q} \rightarrow q_1^0) = (\tilde{q} \rightarrow q_1^0) = (\tilde{q} \rightarrow q\tilde{g})$). Here, we restrict our study to the case $m_{\tilde{g}} > m_{\tilde{q}}$. Due to the unification conditions on the gaugino masses in mSUGRA, this will push the gaugino mass $m_{1=2}$ (and, consequently, the \tilde{g}_1^0 mass) to higher values, when considering larger squark masses.

As a result, in the following we will concentrate on the resonant production of up and down right squarks, \tilde{u}_R and \tilde{d}_R , in the processes

$$\tilde{e}_1^0 + u;d \rightarrow \tilde{u}_R;\tilde{d}_R \rightarrow \tilde{e}_1^0 + u;d; \quad (14)$$

assuming $B(\tilde{u}_R;\tilde{d}_R \rightarrow \tilde{e}_1^0 + u;d) \approx 1$. The dominant signature in the detector will then be given by a strongly interacting particle initiated shower, carrying some relevant fraction of the initial \tilde{e}_1^0 energy.

4 Expected event rate in IceCube

In Table 1, we define the SUSY parameter scenarios we will assume in the following analysis. Starting from the values of $m_0, m_{1=2}$ (with $A_0 = 0$) at the GUT scale, and $\tan\beta, \text{sign}\mu$, all the physical masses and couplings can be calculated at the electro-weak scale by solving a set of renormalization group equations. In order to compute the masses and couplings relevant for our analysis, we have used a computer program as implemented in the package ISAJET [29]. For any of the two Sets (I and II) of $\tan\beta$ and $\text{sign}\mu$ values, we define 5 different scenarios (named as a, b, c, d, e) by varying the common scalar and gaugino masses, m_0 and $m_{1=2}$. The corresponding sets of neutralino, selectron and squark masses are also shown. Masses for squark of different flavors ($u;d;s;c$) are assumed to be degenerate and equal to $m_{\tilde{q}}$. The trilinear soft parameter A_0 is not particularly relevant in the present analysis, and has been set to zero in all cases.

Going from Set I to Set II, scenarios b, c, d, e keep the same m_0 and $m_{1=2}$ values, while the scenario a in Set I is defined by a bit lower $m_{1=2}$ value (150 GeV rather than 170 GeV in Set II), that would not be allowed by present experimental limit in Set II. As a consequence, the scenario a in Set I corresponds to lighter (and easier to produce at the resonance) selectron and squark masses with respect to the scenario a in Set II. For this reason, at the end of our analysis, the Set I will be a bit more favorable as far as allowed event rates are concerned.

m SUGRA -Parameter Scenarios									
		Set I ($\tan \beta = 2; \mu < 0$)				Set II ($\tan \beta = 10; \mu > 0$)			
	m_0	$m_{1=2}$	$m_{\tilde{1}}$	$m_{\tilde{e}_R}$	$m_{\tilde{q}_R}$	$m_{1=2}$	$m_{\tilde{1}}$	$m_{\tilde{e}_R}$	$m_{\tilde{q}_R}$
a	80	150	61	103	331	170	60	110	368
b	150	250	99	179	531	250	93	181	530
c	250	450	178	302	905	450	174	303	905
d	250	170	69	260	432	170	60	261	431
e	350	250	100	363	611	250	94	364	609

Table 1: Definition of different m SUGRA scenarios. In any scenario we set $A_0 = 0$.

On the other hand, one can see that the selectron and squark masses in Set I and II are quite similar in any of the b, c, d, e scenarios. Hence, the eventual independence of our results from the Sets I and II choice will reflect the parameter independence of our results, as discussed in Section 2. The m SUGRA parameter sets in Table 1 take into account the direct-search limits on the particle masses⁶ [22, 23, 30].

In all the scenarios in Set I and II, one has $m_{\tilde{q}_R} < m_{\tilde{g}}$, so that $B(\tilde{q}_R \rightarrow q \tilde{1}) = 1$.

In Figs. 2 a and b, for the parameter Set I and II, respectively, we show (for the a, b, c scenarios) the cross sections for the resonant production of a right selectron and a right squark from the UHE neutralinos scattering on electrons and nucleons, versus the incident neutralino energy.

Note that, as far as one compares different scenarios characterized by a very similar mass spectrum, as happens for scenarios b, c, d, e in the Set I compared to the corresponding ones in the Set II (cf. Table 1), the resulting cross sections do not change sizably. This effect was anticipated in Section 2, and reflects the model independence of scenarios where the resonances are maximally coupled to both the initial and final states, as in the processes $\tilde{1} + f \rightarrow f \rightarrow \tilde{1} + f$ we are considering here.

For comparison, we also present the resonant neutrino cross section for $\nu_e + e \rightarrow W \rightarrow$ all, and the (nonresonant) neutrino-nucleon cross section. The Breit-Wigner W peak cross section corresponds to the incident neutrino energy (E_ν)

$$E_\nu^{\text{peak}} = \frac{M_W^2 - m_e^2}{2m_e}, \quad \frac{M_W^2}{2m_e} \approx 6.4 \cdot 10^6 \text{ GeV} : \quad (15)$$

Cross sections for the resonant squark production do not show the Breit-Wigner structure. Because of the continuous quark momentum distribution inside a nucleon N , any value of the incident neutralino energy larger than a threshold ($E_\nu > \frac{m_q^2 - m^2}{2m_N}$, where m_N is the nucleon mass) can produce a squark at resonance. In this case, the cross section evaluation involves a convolution of the partonic cross section in eq. (6) (with $f = u; d$ and sea quarks) with a parton distribution function $f_q(x; Q^2)$, where x is the momentum fraction of the proton carried away by the parton, and Q is the energy scale at which we evaluate this distribution. The α_R and $\tilde{\alpha}_R$ decay widths are small compared to their masses, and one can substitute the Breit-Wigner propagator in the partonic cross section by a δ -function. Then, the squark-resonance cross section in the $\tilde{1}$ -nucleon scattering becomes:

$$\sigma_{\tilde{q}_R}(E_\nu) = \sum_q \frac{\sigma_{\tilde{q}_R}^{\text{peak}}}{m_{\tilde{q}_R}} x_q f_q(x_q; m_{\tilde{q}_R}^2) \quad (16)$$

⁶The parameter region where the lighter $\tilde{\nu}$ becomes the lightest supersymmetric particle is not considered.

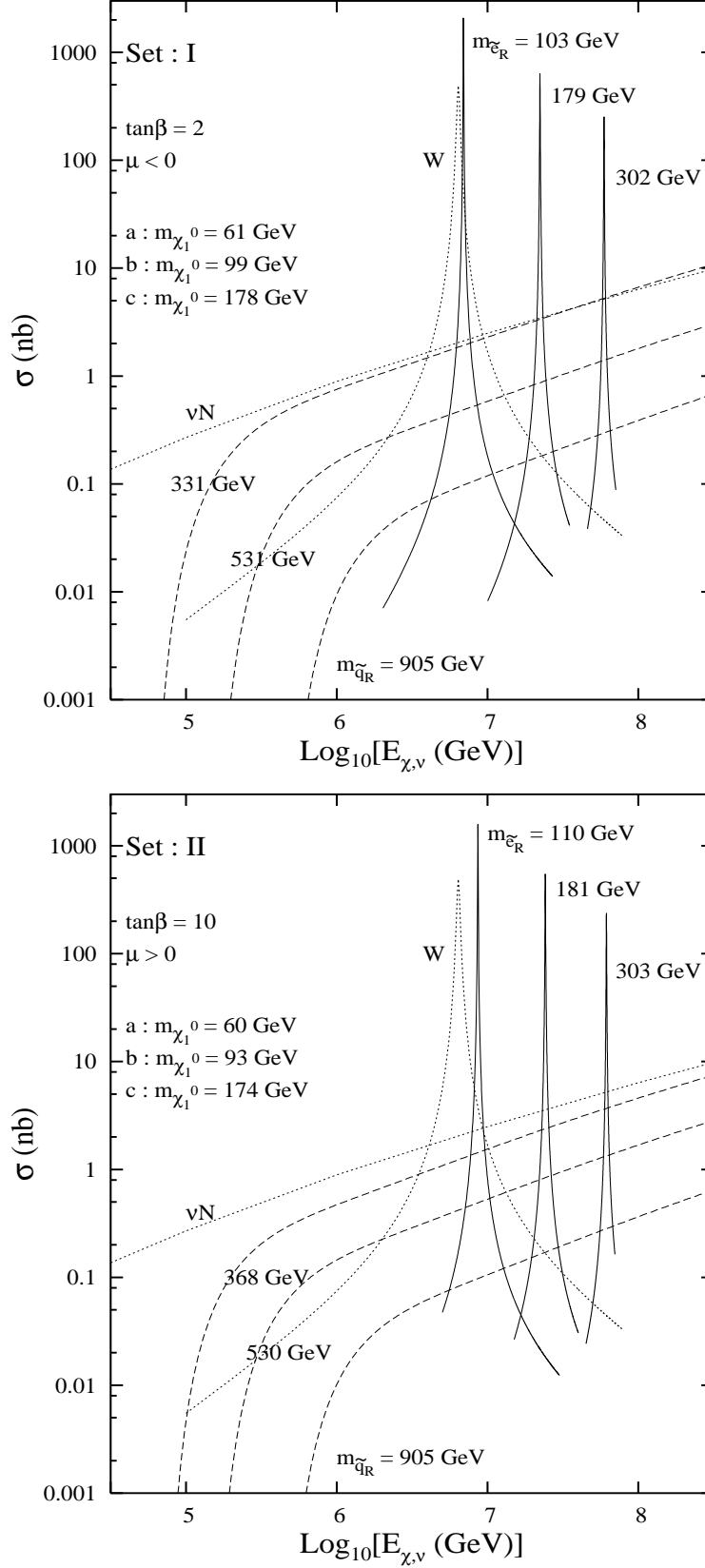


Figure 2: Cross sections (in nb) for electromagnetic (solid curves) and hadronic (dashed curves) final states from UHE neutralino scattering on electrons and nucleons. The dotted lines represent the scattering cross sections of UHE anti-neutrinos on electrons (when marked by W) and on nucleons (when marked by N). The three sets of neutralino, selectron and squark masses correspond to the three scenarios a, b, c in Table 1.

where, $x_q = m_{\tilde{q}_R}^2 = (m_{q_L}^2 + 2 E m_N)$. The summation in eq. (16) is over the u- and d-type quarks (thus including also s and c quarks) in an isoscalar target. In our scenarios, one has $m_{\tilde{u}_R} = m_{\tilde{d}_R} = m_{\tilde{e}_R} = m_{\tilde{s}_R}$ and $\alpha_{\tilde{u}_R} = \alpha_{\tilde{e}_R} = 4 \alpha_{\tilde{d}_R} = 4 \alpha_{\tilde{s}_R}$.

Peak cross sections and total widths relative to all the scenarios defined in Table 1 are presented in Table 2.

The actual event rates N_f can be calculated from the cross section by convoluting it with an appropriate neutralino flux, and multiplying the result by the number of the target electrons/nucleons N_T in a given detector volume, and by the exposure time t , as follows

$$N_f = N_T t \int_{E_{\min}}^Z \sigma_f(E) \frac{dN}{dE} dE ; \quad (17)$$

For selectrons and squarks $\sigma_f(E)$ will be given by eq. (6) and eq. (16), respectively. We assumed the two different neutralino fluxes in eq. (4) and eq. (5). N_T is given by the product of the detector mass (in g units) and Avogadro number (N_A) for nucleons (times 11/18 for electrons).

The selectron width being small compared to its mass (see Table 2), we approximated the Breit-Wigner propagator in eq. (6) by a δ -function. The corresponding expected event number is then

$$N_{e_R} = \epsilon_R \frac{\sigma_{e_R}^{\text{peak}}}{2 m_e} E^{\text{peak}} ; \quad (18)$$

where the factor ϵ_R (depending on the mass of the detector, exposure time and nature of the neutralino flux) includes the product of t , N_T , and the normalization of the fluxes defined in eq. (4) and eq. (5). The exponent sets the shape of the neutralino flux, and is equal to 1.5 and 2, respectively, for the two cases, while E^{peak} , expressed in GeV, is given by eq. (9) where $f \neq e$.

For an ice detector of 1 km^3 and one year of exposure, one has $\epsilon_R = 7.24 \cdot 10^3 [2.29 \cdot 10^7] \text{ nb}^{-1} \text{ GeV}^{-1}$ for the flux in eq. (4) [eq. (5)]. The large difference in the factors is an artifact due to the exponent in the formula above.

For the \tilde{q}_R -resonances, due to the energy distribution of the partons in a nucleon, the number of events will get contributions from a continuous range of incident neutralino energies

$$N_{q_R} = \int_{E_{\min}}^Z \sigma_{q_R}(E) E dE ; \quad (19)$$

where, for a 1-km^3 ice detector and one year of exposure, $\epsilon_R = 3.77 \cdot 10^3 [1.19 \cdot 10^7] \text{ nb}^{-1} \text{ GeV}^{-1}$ for the flux in eq. (4) [eq. (5)], and $\sigma_{q_R}(E)$ is given by eq. (16).

One can note that the peak cross section in eq. (12) is enhanced for small mass differences between the selectron/squark and the neutralino. However, in the product $\sigma_f^{\text{peak}} \frac{dN}{dE}$ that enters the event numbers in eq. (18), and in eq. (19) through eq. (16), the $1 = (m_{\tilde{f}}^2 - m^2)^2$ behavior in σ_f^{peak} is compensated by the resonance-width, that goes as $(m_{\tilde{f}}^2 - m^2)^2$. On the other hand, a residual enhancement associated to the resonance-neutralino mass degeneracy arises from the factor E^{peak} in eq. (18) (cf. eq. (9)), and from the lower limit $E_{\min} = (m_{\tilde{q}}^2 - m^2) = (2m_N)$ of the integral in eq. (19). Hence, selectrons/squarks and neutralinos closer in mass tend to increase the expected event number.

In Table 2, we present the number of events ($N_{e_R; q_R}$), per km^3 per year, expected in an ice detector for the different mSUGRA scenarios defined in Table 1. The number N_{q_R} was always worked out by assuming as lower limit in the integration in eq. (19) the value $E_{\min} = 10^6 \text{ GeV}$ in order to cut off the atmospheric neutrino pollution. In Table 2, the columns corresponding to the number of events have two entries. The first corresponds

to the neutralino flux defined in eq. (4) (Fragmentation-like), while the second (shown in parenthesis) assumes the flux in eq. (5) (Fermi-like).

Number of events (Set I : $\tan \beta = 2; \mu < 0$)									
	$m_{\tilde{L}_1}$ (GeV)	$m_{\tilde{e}_R}$ (GeV)	$m_{\tilde{q}_R}$ (GeV)	$\sigma_{\tilde{e}_R}$ (GeV)	$\sigma_{\tilde{q}_R}^{\text{peak}}$ (nb)	$N_{\tilde{e}_R}$ ($=\text{km}^3\text{-yr}$)	$\sigma_{\tilde{q}_R}$ (GeV)	$\sigma_{\tilde{q}_R}^{\text{peak}}$ (nb)	$N_{\tilde{q}_R}$ ($=\text{km}^3\text{-yr}$)
a	61	103	331	0.215	2170	19 (23)	0.685	95.62	16.52 (15.34)
b	99	179	531	0.43	634	3.36 (2.26)	1.104	37.22	4.28 (3.77)
c	178	302	905	0.643	254	0.78 (0.32)	1.871	12.92	0.86 (0.64)
d	69	260	432	1.11	167	0.70 (0.28)	0.912	55.16	7.79 (7.04)
e	100	363	611	1.55	86	0.26 (0.08)	1.291	27.65	2.84 (2.44)

Number of events (Set II : $\tan \beta = 10; \mu > 0$)									
	$m_{\tilde{L}_1}$ (GeV)	$m_{\tilde{e}_R}$ (GeV)	$m_{\tilde{q}_R}$ (GeV)	$\sigma_{\tilde{e}_R}$ (GeV)	$\sigma_{\tilde{q}_R}^{\text{peak}}$ (nb)	$N_{\tilde{e}_R}$ ($=\text{km}^3\text{-yr}$)	$\sigma_{\tilde{q}_R}$ (GeV)	$\sigma_{\tilde{q}_R}^{\text{peak}}$ (nb)	$N_{\tilde{q}_R}$ ($=\text{km}^3\text{-yr}$)
a	60	110	368	0.255	1608	12.88 (13.86)	0.756	76.19	12.02 (11.04)
b	93	181	530	0.48	550	3.39 (3.04)	1.098	37.05	4.25 (3.75)
c	174	303	905	0.68	236	0.72 (0.30)	1.868	12.87	0.85 (0.64)
d	60	261	431	1.12	150	0.62 (0.24)	0.905	54.73	7.69 (6.95)
e	94	364	609	1.56	84	0.26 (0.08)	1.285	27.66	2.83 (2.43)

Table 2: Number of events from selectron and squark resonant production for the scenarios listed in Table 1. We also show the resonance decay widths and peak cross sections. The first of the two entries in the event-rate columns corresponds to the number of events calculated with a Fragmentation neutralino flux in eq. (4), while the second (in parenthesis) follows from Fermi at spectrum in eq. (5). While calculating the squark event rates a incident neutralino energy threshold of 1 PeV is used.

Number of events from UHE ν_μ interaction		
$W \rightarrow e e$	$W \rightarrow \text{hadrons}$	$P_i (i + i)_{CC+NC}$
2 (2.5)	12 (15)	55 (56)

Table 3: Number of events from UHE ν_μ , CC and NC interaction in IceCube per year. Rates are calculated using for the UHE ν_μ 's a Fragmentation flux in eq. (4), while the numbers in the parenthesis are calculated using the Fermi at flux in eq. (5). An incident-neutrino energy threshold of 1 PeV is used.

For comparison the expected event rates from the resonant W production from $\nu_e e$ scattering, in the hadronic and leptonic channels, are presented in Table 3 for the flux in eq. (4) [eq. (5)]. Since the fluxes defined before are relative to one flavor of $\nu + \bar{\nu}$, assuming a complete neutrino flavour mixing due to non-zero neutrino masses, we use a ν_e flux that is half of those defined in eq. (4) [eq. (5)]. We also presented total $\bar{\nu}N$ and $\bar{\nu}N$ charged current (CC) plus neutral current (NC) event rates.

In the scenario a, where the resonance masses are quite close to the present experimental limit, one has about 19-23 leptonic events for $\tan\beta = 2$; $\mu < 0$, and 13-14 events for $\tan\beta = 10$; $\mu > 0$, depending on the assumed neutralino flux (the difference between the two Sets being due mostly to the different physical masses). From the hadronic channel, one expects 15-17 events in the first case, and 11-12 events in the second. Of course, the rates go down when increasing the resonance masses. Anyway, one can have more than 2 squark event for $m_{\tilde{q}_R} > 600$ GeV (cf. scenarios b, d, e).

With the assumed neutralino fluxes, one could detect some SUSY effect in IceCube for scalar masses not too far from their present experimental limits. However, as we have discussed in Section 1, the normalization of the fluxes in eq. (4) and eq. (5) are quite conservative. For instance, one is presently allowed to assume normalizations as large as at least a few times the ones adopted here without violating any experimental constraint. Indeed, one is allowed to take a flux as large as: $E^2 \frac{dN}{dz} = 4 \cdot 5 \cdot 10^{-7} \text{ GeV cm}^{-2} \text{ s}^{-1} \text{ sr}^{-1}$ [27]. This would make the number of events higher and better detectable.

Although in our study we included the complete treatment of all parameters, starting from the scale M_{GUT} according to the mSUGRA model, the outcome of our study confirms that in the scenarios considered (that are quite general for the leptonic sector, and are mainly characterized by a gluino heavier than a right squark as far as the hadronic sector is concerned) the event rates associated to the right scalar resonances change mainly following the pattern of physical masses, independently from other parameters. This is a nice feature of the present analysis, that makes the study quite model independent.

5 Disentangling the neutralino signal by neutrino calibration

We will now briefly address the problem of the effective visible-energy spectrum coming from the two body decays $\tilde{\nu}_R \rightarrow \nu_1^0$, that is of course a crucial characteristic in the detection of a resonance signal.

In the resonant $\tilde{\nu}_R$ decay into an electron plus an invisible neutralino ν_1^0 , only the electron energy contributes to the visible energy. In Fig. 3, we plot the visible-energy spectrum $z \frac{dN}{dz}$ (where $z = \log_{10} E_{\text{vis}}$, and $z = 0.1$ assumes a 10% experimental sensitivity) corresponding to the resonant $\tilde{\nu}_R$ production and decay into ν_1^0 . For comparison, we also show the visible-energy spectrum for a resonant W decaying into either e or hadrons. When the W decays hadronically, the total energy of the initial incident neutrino transfers to some visible energy in the final state. Hence, the $z \frac{dN}{dz}$ spectrum has a resonant structure corresponding to the initial neutrino energy $E = m_W^2 = (2m_e)^2 \approx 6.4 \cdot 10^6 \text{ GeV}$. On the other hand, when the W decays leptonically, only a fraction of the incident neutrino energy goes into visible energy whose distribution is characteristic of a two-body decay, just as in the $\tilde{\nu}_R \rightarrow \nu_1^0$ case. The positions of the sharp end points of the spectra are determined by the masses of the resonance and of the decay products. They provide a handle to differentiate between the visible energy coming from a W decay and a $\tilde{\nu}_R$ decay. The position of the visible-energy peak for the hadronic W decay, and edge for the leptonic W decay is of course well known.

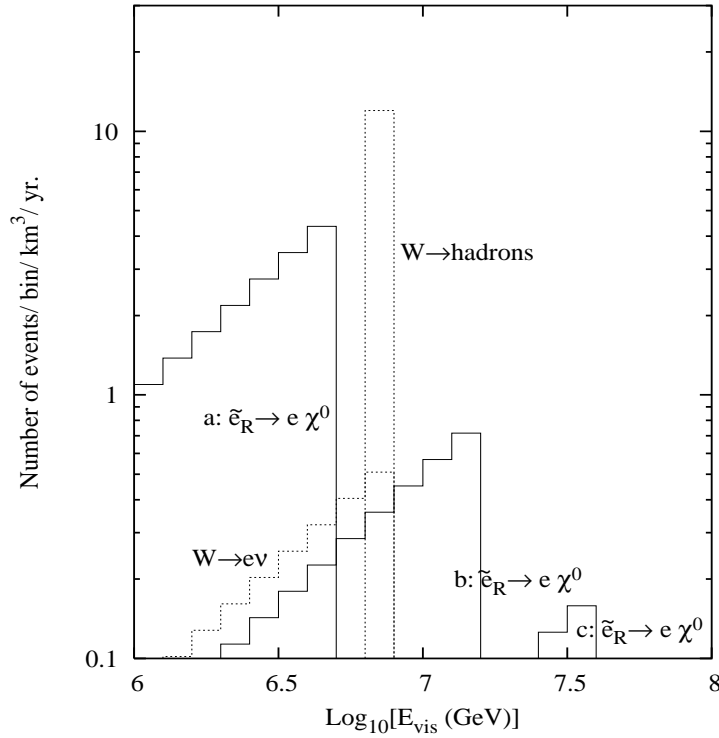


Figure 3: Visible energy spectra of the resonance decay products calculated with a Fragmentation neutralino flux in eq. 4. The dotted histograms represents the electron energy spectrum (marked with $W \rightarrow e$) and hadronic energy spectrum (marked with $W \rightarrow \text{hadrons}$) coming from resonant W production and decay to the corresponding channels. The three distributions (solid lines) marked with $e_R \rightarrow e \chi^0$ represent the first three scenarios of Set I in Table 1, for $\tan \beta = 2$; $\mu < 0$. The neutralino flux in eq. (4) has been assumed.

In particular, the hadronic W decay defines a sharply clustered group of events [about 12 for the Fragmentation spectrum, and 15 for the Fermi-like power law], whose intensity may be correlated with the two electromagnetic channels arising from $W \rightarrow e + e$ [2 (2.5)] and $W \rightarrow \mu + \mu$ [2 (2.5)] events. The other decay channel $W \rightarrow \tau + \tau$ [2 (2.5) events] is not delivering more than a single PeV muon track, quite difficult to fully recognize. The electron and electromagnetic energy spectra are not monochromatic, but are growing linearly with energy up to the $E = 6.4$ PeV threshold. The average electron (tau) energy is nearly half (a third) of the hadronic-channel energy. The distribution is spread according to a continuous power law as shown in Fig. 3. The birth and decay will be in general source of a characteristic double-bang event [31]. Hence, in the case the event rate for the e_R production is sufficiently high, the appearance of a sharp edge at some different energy (away from the W hadronic, electronic, and tau bumps) could point to some new physics corresponding to a resonant e_R production from UHECR neutralinos. At the moment, such reconstruction seems possible mainly for a neutralino flux just below or comparable to present lower bounds on neutrino fluxes, while selectron resonance masses should not be too far from the present experimental limits.

The mass ranges considered are of great astrophysical interest, and within the reach of the CERN LHC. A near-future underground τ -detector could then cross-check a possible SUSY discovery at future colliders.

6 The role of the sneutrino burst

The resonant production of Z -bosons via UHE scattering of massive relic neutrinos has been the backbone of the so called Z -burst mechanism [16] that could explain the GZK puzzle. UHE neutrinos in Z -burst are the messengers able to overcome the GZK cut-off, by opening a link between UHECR and most distant cosmic sources. About 70% of the Z -bosons decays hadronically, thus producing protons, neutrons and anti-nucleons as well as pions (and consequent photons from neutral-pions decays). The Z -decay products could have quite naturally energies beyond the GZK scale for appropriate relic neutrino masses, since $E' \approx M_Z^2 = (2m_e)^2 \approx 4 \cdot 10^6 \frac{0.51\text{eV}}{m} \text{ eV}$, which corresponds to $E_p \approx \frac{1}{20} M_Z^2 = (2m_e)^2$. If relic neutrino halos are present at distances less than about 50 Mpc ⁷, then these protons or anti-protons (or photons) could arrive to the earth atmosphere without much energy loss. Consequently, air-showers produced by these extremely high-energy nucleons could give rise to the super GZK events, as detected by the AGASA experiment [3]. Crucial ingredients of this picture are of course sufficiently large UHE-neutrino fluxes and relic-neutrino densities in the Local Group or Super Galactic Plane. Then, the Z -burst model has a good potential for explaining observed correlation of UHECR arrivals from BL-Lac sources at distances well above GZK, and electron pair losses [5].

In this section, we will consider the resonant sneutrino ($\tilde{\nu}$) production from the UHE neutralinos scattering off relic neutrinos, and its subsequent decay into visible final states

$$\tilde{\nu}_1^0 \rightarrow \tilde{\nu} + X_{\text{vis}}; \quad (20)$$

where X_{vis} stands for the all final states with at least one visible particle. In particular, we will discuss whether this process can have a role similar to the Z -burst one in the observed component of the cosmic-ray spectrum beyond the GZK energy.

The channel in eq. (20) differs from the resonant selectron and squark production previously analyzed under various aspects. First, due to the lightness of the target mass, it requires much larger $\tilde{\nu}_1^0$ energies according to eq. (9). Second, optimizing cross sections by considering scenarios where the sneutrino is maximally coupled to the initial state, and, at the same time, it decays into the initial particles $\tilde{\nu} \rightarrow \tilde{\nu}_1^0$ (as done for the selectron and squark resonances) is not viable, since this would give rise to invisible final states. On the other hand, the sneutrino can decay into heavier neutralinos $\tilde{\nu}_i^0$ ($i = 2, 3, 4$) and charginos $\tilde{\chi}_j^\pm$ ($j = 1, 2$). The subsequent neutralino and chargino decays into hadrons and leptons might produce highly energetic protons, pions and electrons that would be able to initiate the super GZK air showers. Looking back at eq. (6) for the cross section, one is interested in scenarios where neither $B(\tilde{\nu} \rightarrow \tilde{\nu}_1^0)$ nor $B(\tilde{\nu} \rightarrow X_{\text{vis}})$ is small. The latter are complementary quantities [we will check that one can assume quite accurately $B(\tilde{\nu} \rightarrow X_{\text{vis}}) \approx 1 - B(\tilde{\nu} \rightarrow \tilde{\nu}_1^0)$]. Hence, the sneutrino production cross section is automatically penalized. Furthermore, the rates will be in general quite model dependent. Our results will not be simply determined by the particle mass spectrum (as in the right selectrons/squarks production), but will depend also on the couplings (and on the $\tan\beta$ and μ parameters) in a nontrivial way. Finally, since a visible sneutrino channel can arise from a decay chain, the energy of the visible decay products can in principle be quite depleted. In the following, we will also discuss the sneutrino energy flow in the visible decay products.

The sneutrino branching fraction into visible final states $B(\tilde{\nu} \rightarrow X_{\text{vis}})$ is in general made

⁷The distances of the center of dense clusters from the earth are estimated to be 16 Mpc for Virgo, while our Super-Galactic Plane diameter is about 50 Mpc [32].

$\tan \beta = 2; \mu > 0; A_0 = 0$												
	m_0	$m_{1=2}$	$m_{\tilde{\nu}}$	$m_{\tilde{\chi}_1^0}$	$m_{\tilde{\chi}_2^0}$	$m_{\tilde{\chi}_1^\pm}$	$\tilde{\nu}$	$B_{\tilde{\chi}_1^0}$	$B_{\tilde{\chi}_2^0}$	$B_{\tilde{\chi}_1^\pm}$	peak $\tilde{\nu}$	peak $\tilde{\nu}$
a'	80	170	132	57	108	104	0.37	0.52	0.10	0.38	212	78.4
b'	150	250	220	92	175	174	0.60	0.42	0.17	0.41	64	38.4
c'	250	450	387	174	340	340	0.59	0.58	0.14	0.28	25	14.7
d'	250	170	269	59	112	110	2.53	0.19	0.21	0.59	22	55.6
e'	350	250	383	93	179	178	3.29	0.16	0.26	0.58	10.2	33.5

Table 4: Relevant mass spectrum, widths, branching fractions and peak cross sections for 5 sneutrino scenarios. All masses and decay widths are in GeV, and $\sigma_{\tilde{\nu}}^{\text{peak}}$ is in nb.

up of different components

$$B(\tilde{\nu} \rightarrow X_{\text{vis}}) = \sum_{j=1}^2 X_j^2 B(\tilde{\nu} \rightarrow l_j) + \sum_{i=2}^4 X_i^4 B(\tilde{\nu} \rightarrow \tilde{\chi}_i^0) B(\tilde{\chi}_i^0 \rightarrow f f) + B(\tilde{\nu} \rightarrow \tilde{\chi}_1^0) \quad (21)$$

where $f \in e, \mu, \tau$.

The $\tilde{\nu}$ decays into the second neutralino $\tilde{\chi}_2^0$ and into the lightest chargino $\tilde{\chi}_1^\pm$ are in general dominant. The subsequent decays $\tilde{\chi}_1^0 \rightarrow q\bar{q}$ (with a branching ratio of about 66 %) and $\tilde{\chi}_1^\pm \rightarrow l_\pm \tilde{\nu}$ (with a branching ratio of about 33 %) are the sources of hadrons and charged leptons, respectively, that may trigger the highest-energy air showers. The second neutralino can have a substantial decay rate into the invisible channel $\tilde{\chi}_2^0 \rightarrow \tilde{\chi}_1^0$. Otherwise, a $\tilde{\chi}_2^0$ decay produces quarks and leptons via $\tilde{\chi}_2^0 \rightarrow q\bar{q}; ll$. The $\tilde{\chi}_2^0 \rightarrow e\bar{e}$ decay may also be kinematically allowed (e.g., this happens for the input parameters in the scenario a' of Table 4). In the latter case, no hadron arises from the decay chain.

The presence of a heavy invisible particle ($\tilde{\chi}_1^0$) among the $\tilde{\nu}$ decay products makes the visible part of the spectrum quite different from the Z-burst case. The results are in general model dependent and less promising, and the incoming UHE $\tilde{\nu}$ energy should be at higher energies. Indeed, the decay kinematics of a Z-burst event is quite simple. The hadrons resulting from the $Z \rightarrow q\bar{q}$ decay carry away all the energy of the incident UHE neutrino (i.e., the Z resonance energy). On the other hand, the average energy of the visible sneutrino decay products is quite lower than the sneutrino mass, since hadrons can only appear either from a three-body decay of $\tilde{\chi}_2^0 \rightarrow \tilde{\chi}_1^0 + \text{hadrons}$, or from a two-body decay chain $(\tilde{\chi}_2^0 \rightarrow \tilde{\chi}_1^0 + Z(W) \rightarrow \text{hadrons})$ following the initial two-body $\tilde{\nu}$ decay. Sneutrino masses, anyway, can be quite heavier than the Z mass, and this could compensate partly the depletion of the energy spectrum of the sneutrino decay products, that in any case would have a less resonant structure than in Z-burst case.

The detailed energy spectrum of the hadrons and leptons coming from the sneutrino decay cascades also depends crucially on the masses of the particles in each step of the decay chains. Their study would require a Monte Carlo treatment of the complete kinematics. We will not go into this analysis here.

The observed event number is ruled by the product $\sigma_{\tilde{\nu}}^{\text{peak}} \times \mathcal{L}$, the peak cross section times the resonance width, as well as by the sneutrino branching fractions into the initial and final states. In Table 4, we present these quantities for 5 different scenarios (named a', b', c', d', e'), when $\tan \beta = 2; \mu > 0$; and $A_0 = 0$. These scenarios differ by the ones of Set I in Table 1 only for the positive sign of μ , since $\mu > 0$ somehow optimizes the sneutrino signal. For example, for $\mu < 0$, a visible sneutrino is kinematically disallowed when $m_0 = 80$ GeV and $m_{1=2} = 170$ GeV. For higher values of $\tan \beta$ (≥ 10), the spectrum of physical masses would not be much affected. However, due to the smaller couplings of the sneutrino to $\tilde{\chi}_{1,2}^0$

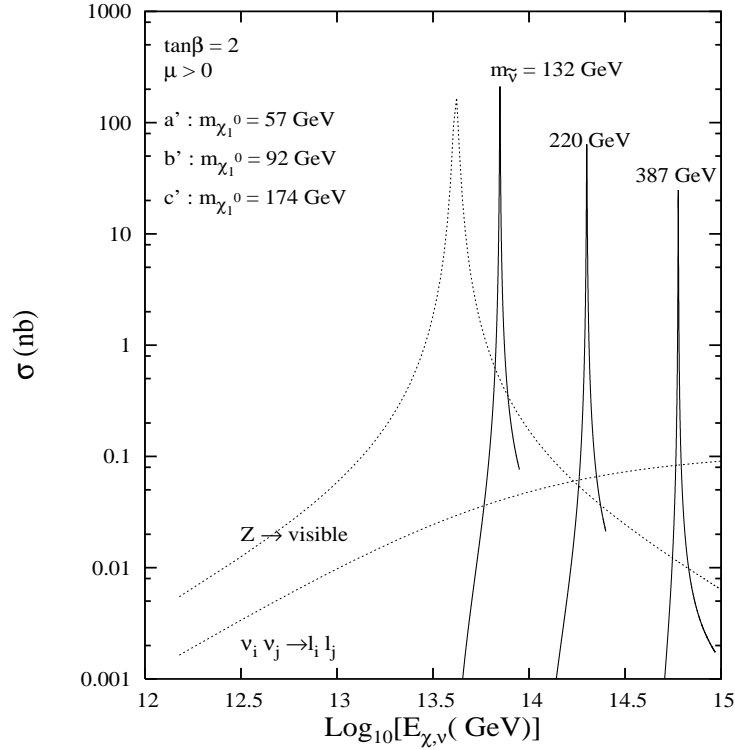


Figure 4: Cross sections (in nb) for resonant sneutrino production and visible decay (solid curves) from UHE neutralino scattering on relic neutrinos. The dotted lines represent the scattering cross section of UHE neutrinos on relic neutrinos producing a Z -boson at resonance (when marked by $Z \rightarrow \text{visible}$), and the continuum cross section for $\nu_i \nu_j^{\text{relic}} \rightarrow l_i l_j$ (when marked by $\nu_i \nu_j \rightarrow l_i l_j$). We assumed a relic-neutrino mass $m = 0.1$ eV. The three sets of neutralino and sneutrino masses correspond to the first three scenarios in Table 4.

and χ_1 , the sneutrino decay width would decrease, resulting into a smaller $\sigma_{\tilde{\nu}}^{\text{peak}}$ value⁸.

In all the scenarios considered in Table 4, the $m_{\tilde{\nu}}$ is too light for allowing the sneutrino to decay into heavier charginos and $\chi_{3,4}^0$. This is important in order not to deplete too much B ($\sim \chi_1^0$) and, as a consequence, the sneutrino cross section.

In Fig. 4, we plot the cross sections for the resonant $\tilde{\nu}$ production in the channel in eq. (20) versus the incident neutralino energy, for the three scenarios a', b', c' defined in Table 4. The cross section for the Z -production from UHE- scattering on relic neutrinos is also shown versus the incident neutrino energy, for comparison. A relic neutrino mass of 0.1 eV is assumed in all cases [33] and the resonant incoming UHE neutralino energy is given by $E^{\text{peak}}_{\tilde{\nu}} = \frac{m_{\tilde{\nu}}^2 - m_{\chi_1^0}^2}{2m_{\tilde{\nu}}}$.

One can note that, although the sneutrino peak cross section can be close to (and even higher than) the Z peak cross section into visible final states ($\sigma_Z^{\text{peak}} \sim 185$ nb), the sneutrino width in scenarios a', b', c' is quite smaller than the Z total width $\Gamma_Z \sim 2.5$ GeV (cf. Table 4). In the most favorable scenario (a'), one reaches $\sigma_{\tilde{\nu}}^{\text{peak}} \sim 78$ nb GeV, to be compared with $\sigma_Z^{\text{peak}} \sim 463$ nb GeV. While calculating the peak cross sections, in both the Z and $\tilde{\nu}$ cases the relic light neutrinos are assumed to be Dirac fermions. In case of Majorana neutrinos, the peak cross sections are enhanced by a factor 2, doubling the

⁸For instance, for the best case presented in Table 4 (first row), $m_{\tilde{\nu}}$ goes down to 0.21 GeV, if we take $\tan\beta = 10$, with $\sigma_{\tilde{\nu}}^{\text{peak}}$ shifting to 240 nb.

number of the events in each case.

Of course, the latter comparison makes sense only when assuming a comparable flux of incident neutrinos and neutralinos. Assuming equal fluxes, an extra fraction of sneutrino events could add to the Z-burst counting, presumably with a bit less structured energy distribution. Further in-depth analysis will be needed to establish the latter point.

7 Conclusions

If elementary-particle interactions are governed by supersymmetry, then an important component of the UHECR may be given by the lightest stable supersymmetric particle, namely the lightest neutralino. Some of the models trying to explain the UHECR spectrum beyond the GZK cut-off via superheavy particle decays, when including supersymmetry, predict a flux of UHE neutralinos arriving to the earth. One of the major challenges of the future cosmic-ray experiments is to verify such predictions. In this paper, we computed the event rates for right selectrons and right squarks produced on resonance, when UHE neutralinos scatter off the electrons and quarks in a detector like IceCube. We assumed a well-motivated model of supersymmetry, that is minimal supergravity. We argued that, inside this framework, where one has in general $B(\tilde{e}_R \rightarrow e \tilde{\chi}_1^0) \sim 1$, and (for gluinos heavier than squarks) $B(\tilde{q}_R \rightarrow q \tilde{\chi}_1^0) \sim 1$, the results are quite model independent. This means that the relevant phenomenology depends only on the physical masses assumed for the right scalars and neutralinos, that are governing kinematics effects. Any other parameter dependence, such as the one arising from the neutralino physical compositions and couplings, drops out.

Two different phenomenological forms for the neutralino fluxes were assumed to calculate the event rates: a Fragmentation power law, and a Fermi flat spectrum. We set the flux normalization on the basis of present bounds on the UHE neutrino flux from the AGASA and Fly's Eye experiments (assuming, quite conservatively, that interaction rates of neutrino and neutralino with matter are of comparable strength). For comparison, event rates for resonant W production in UHE anti-neutrino scattering off electrons in matter were also presented. We showed here for the first time a detailed spectrum of the visible energy released in the $\tilde{e}e$ reaction in underground detectors. We showed how to calibrate through the W resonance all the other neutrino flavors and the SUSY signals. The event rates for SUSY particle resonances are found to be comparable with those for the W production only for selectron and squark masses quite close to their present experimental bounds. Other signatures in different scenarios will be discussed elsewhere.

We also considered the possibility of resonant production of sneutrinos in the interaction of UHE neutralinos with light relic neutrinos in the extended Galactic or Local Group hot neutrino halo. The visible decay products of the sneutrinos might trigger air-showers beyond GZK energies, thus mimicking the so called Z-burst phenomenon. However, even in the most promising scenarios, we found that the sneutrino-burst event rate would be 5-6 times smaller than the Z-burst rate (assuming similar fluxes for UHE neutrinos and neutralinos). Furthermore, the UHE neutralino energies tuned for such a sneutrino-burst are usually higher than Z-burst ones, making it less attractive than the standard Z-burst model.

In conclusion, we found a well-defined and interesting window of MUGRA parameters that can be tested by the next-generation underground detectors. The corresponding signal may exceed in some cases the standard neutrino ones. Its imprint may be disentangled in a realistic way. These high-energy astrophysical traces are offering a new opportunity to high-energy astrophysics to anticipate SUSY discovery at colliders.

Acknowledgments

This work was partially supported by the RTN European Programme MRTN-CT-2004-503369 (Quest for Unification).

References

- [1] K. G. Reisen, Phys. Rev. Lett. 16 748 (1966) ; G. Zatspin, V. Kuzm in, Pisma Zh. Eksp. Teor. Fiz. 4 114 (1966) [JETP Lett. 4 78 (1966)].
- [2] Fly's Eye Collab., D. Bird et al., Astrophys. J. 441 144 (1995).
- [3] AGASA Collab., H. Hayashida et al., Astropart. Phys. 10 303 (1999).
- [4] A. Zech for the Hires Collab., astro-ph/0409140 .
- [5] D. Gorbunov, P. Tinyakov, I. Tkachev and S. Troitsky, Astrophys. J. 577 L93 (2002); D. Fargion, A. Colaïuda, astro-ph/0409022.
- [6] For a comprehensive review see, P. Bhattacharjee, G. Sigl, Phys. Rept. 327, 109 (2000).
- [7] L. Anchordoqui, T. Paul, S. Reucroft and J. Swain, Int. J. Mod. Phys. A 18 2229 (2003); D. Torres, L. Anchordoqui, astro-ph/0402371 and references therein.
- [8] C. T. Hill, Nucl. Phys. B 224, 469 (1983); C. T. Hill, D. N. Schramm and T. P. Walker, Phys. Rev. D 36, 1007 (1987); P. Bhattacharjee, C. T. Hill and D. N. Schramm, Phys. Rev. Lett. 69, 567 (1992); V. Berezinsky, X. Martin and A. Vilenkin, Phys. Rev. D 56, 2024 (1997); L. M. Asperi and G. A. Silva, Astropart. Phys. 8, 173 (1998); L. M. Asperi and M. Orsaria, Astropart. Phys. 16, 411 (2002); V. Berezinsky and A. Vilenkin, Phys. Rev. Lett. 79, 5202 (1997); V. Berezinsky, M. Kachelriess and A. Vilenkin, Phys. Rev. Lett. 79, 4302 (1997); V. A. Kuzm in and V. A. Rubakov, Phys. Atom. Nucl. 61, 1028 (1998) [Yad. Fiz. 61, 1122 (1998)]; P. Jaikumar and A. Mazumdar, Phys. Rev. Lett. 90, 191301 (2003); M. Birkel and S. Sarkar, Astropart. Phys. 9, 297 (1998); Z. Fodor and S. D. Katz, Phys. Rev. Lett. 86, 3224 (2001); C. Coriano, A. E. Faraggi and M. Plumacher, Nucl. Phys. B 614, 233 (2001).
- [9] V. Berezinsky, M. Kachelriess, Phys. Lett. B 422 162 (1998).
- [10] V. Berezinsky, M. Kachelriess, Phys. Lett. B 434 61 (1998); V. Berezinsky, M. Kachelriess and S. Ostapchenko, Phys. Rev. D 65 083004 (2002); A. Ibarra, R. Toldra, Jour. High Energy Phys. 0206:006 (2002) ; R. Abisio, V. Berezinsky and M. Kachelriess, Phys. Rev. D 64 094023 (2004)
- [11] S. Sarkar and R. Toldra, Nucl. Phys. B 621 495 (2002).
- [12] C. Barbot, M. Drees, Phys. Lett. B 533 107 (2002); C. Barbot, M. Drees, F. Halzen and D. Hooper, Phys. Lett. B 563 132 (2003); C. Barbot, hep-ph/0308028.
- [13] V. Dubrovich, D. Fargion, and M. Khlopov, hep-ph/0312105.
- [14] For a review, see H. E. Haber and G. L. Kane, Phys. Rept. 117, 75 (1985).
- [15] For a recent review, see B. Mile, hep-ph/0407204.

- [16] D. Fargion, B. Mele and A. Salis, *Astrophys. J.* 517 725 (1999); T. Weiler, *Astropart. Phys.* 11 303 (1999).
- [17] L. Anchordoqui, H. Goldberg and P. Nath, *Phys. Rev. D* 70 025014 (2004).
- [18] O. Catalano, *Nuovo. Cim.* 24C 445 (2001); L. Scarsi, *Nuovo. Cim.* 24C 471 (2001).
- [19] D. Fargion [astro-ph/9704205](#); *Astrophys. J.* 570 909 (2002).
- [20] D. Fargion, P. De Sanctis Lucentini, M. De Santis and M. Grossi, *Astrophys. J.* 613 1285 (2004).
- [21] See for example, J. Alvarez-Muniz and F. Halzen, *AP Conf. Proc.* 579, 305 (2001); [astro-ph/0102106](#).
- [22] LEP2 SUSY Working Group, Combined LEP Selectron/Smuon/Stau Results, 183-208 GeV, ALEPH, DELPHI, L3, OPAL Experiments, [LEP SUSY WG/04-01.1](#)
- [23] T. Aolder et al., The CDF Collab., *Phys. Rev. Lett.* 88, 041801 (2002)
- [24] S.L. Glashow, *Phys. Rev.* 118, 316 (1960).
- [25] A. Chamseddine, H. Arnowitt and P. Nath, *Phys. Rev. Lett.* 49 970 (1982); R. Barbieri, S. Ferrara and C. Savoy, *Phys. Lett. B* 119 343 (1982); L. Hall, J. Lykken and S. Weinberg, *Phys. Rev. D* 27 2359 (1983); A. Chamseddine, H. Arnowitt and P. Nath, *Nucl. Phys. B* 227 121 (1983).
- [26] J. Ellis, K. Olive, Y. Santoso and V. Spanos, *Phys. Lett. B* 565 176 (2003); U. Chattopadhyay, A. Corsetti and P. Nath, *Phys. Rev. D* 68 035005 (2003).
- [27] See the talk by K. Woschnagg at Neutrino 2004 conference, Paris; also see M. Ackermann for the AMANDA Collab., [astro-ph/0405218](#).
- [28] I. Kravchenko, [astro-ph/0306408](#).
- [29] F. Paige, S. Protopescu, H. Baer and X. Tata, [hep-ph/0312045](#).
- [30] For the lower mass limits on neutralinos and charginos see: ALEPH Collab. D. Abbaneo et al., [CERN-EP/2003-077](#).
- [31] J. Leamed, S. Pakvasa, *Astropart. Phys.* 3 267 (1995).
- [32] For example, see P. Fouque, J. M. Solanes, T. Sanchis and C. Balkowski, "Structure, mass and distance of the Virgo cluster from a Tolman-Bondi model", [arXiv:astro-ph/0106261](#).
- [33] S. Hannestad, [hep-ph/0409108](#).